



Interference Aware Inter-Cell Rank Coordination for 5G Systems

Mahmood, Nurul Huda; Pedersen, Klaus I.; Mogensen, Preben Elgaard

Published in:
IEEE Access

DOI (link to publication from Publisher):
[10.1109/ACCESS.2017.2672799](https://doi.org/10.1109/ACCESS.2017.2672799)

Publication date:
2017

Document Version
Publisher's PDF, also known as Version of record

[Link to publication from Aalborg University](#)

Citation for published version (APA):
Mahmood, N. H., Pedersen, K. I., & Mogensen, P. E. (2017). Interference Aware Inter-Cell Rank Coordination for 5G Systems. *IEEE Access*, 5, 2339 - 2350. <https://doi.org/10.1109/ACCESS.2017.2672799>

General rights

Copyright and moral rights for the publications made accessible in the public portal are retained by the authors and/or other copyright owners and it is a condition of accessing publications that users recognise and abide by the legal requirements associated with these rights.

- Users may download and print one copy of any publication from the public portal for the purpose of private study or research.
- You may not further distribute the material or use it for any profit-making activity or commercial gain
- You may freely distribute the URL identifying the publication in the public portal -

Take down policy

If you believe that this document breaches copyright please contact us at vbn@aub.aau.dk providing details, and we will remove access to the work immediately and investigate your claim.

Received January 10, 2017, accepted February 3, 2017, date of publication February 22, 2017, date of current version March 15, 2017.

Digital Object Identifier 10.1109/ACCESS.2017.2672799

Interference Aware Inter-Cell Rank Coordination for 5G Systems

NURUL HUDA MAHMOOD¹, KLAUS INGEMANN PEDERSEN^{1,2}, AND PREBEN MOGENSEN^{1,2}

¹Wireless Communications Networks Section, Department of Electronic Systems, Aalborg University, 9220 Aalborg, Denmark

²Nokia Bell Labs, 9220 Aalborg, Denmark

Corresponding author: N. H. Mahmood (fuadnh@ieee.org)

This work was supported by the European Union through the Horizon 2020 Project FANTASTIC-5G under Grant ICT-671660.

ABSTRACT Multiple transmit and receive antennas can be used to increase the number of independent streams between a transmitter–receiver pair, and/or to improve the interference resilience with the help of linear minimum mean squared error (MMSE) receivers. Typically, rank adaptation algorithms aim at balancing the tradeoff between increasing the spatial multiplexing gain through independent streams, and improving the interference resilience property. An interference aware inter-cell rank coordination framework for the future fifth generation wireless system is proposed in this paper. The proposal utilizes results from random matrix theory to estimate the mean signal-to-interference-plus-noise ratio at the MMSE receiver. In addition, a game-theoretic interference pricing measure is introduced as an inter-cell interference management mechanism to balance the spatial multiplexing versus interference resilience tradeoff. Centralized and distributed implementations of the proposed inter-cell rank coordination framework are presented, followed by exhaustive Monte Carlo simulation results demonstrating its performance. The obtained results indicate that the performance of the proposed method is up to 56% better than conventional non interference-aware schemes; and within 6% of the optimum performance obtained using a brute-force exhaustive search algorithm though it incurs much lower computational complexity.

INDEX TERMS Rank adaptation, 5G, MMSE receivers, MIMO, random matrix theory, interference pricing.

I. INTRODUCTION

The first half of this decade saw the emergence of the fifth generation cellular technology (5G) as a concept. Demand for radically higher data rates, increased reliability and improved energy efficiency drives the 5G standard to adopt a number of novel technologies, primarily through a combination of gains in three frontiers: moving to higher frequencies, cell densification, and harnessing multiple input multiple output (MIMO) capabilities [1]. However, early 5G systems will most likely enhance the spectral efficiency through small cell and MIMO since operation in higher frequencies like the millimeter wave (mmWave) spectrum is yet to mature for commercial applications [2].

Interference is a fundamental element of wireless systems, and has to be mitigated efficiently, especially in dense networks [3]. Interference coordination is heavily featured in the fourth generation/long term evaluation (LTE) system. Inter-Cell Interference Coordination (ICIC) [4] and enhanced ICIC (eICIC) [5] in LTE systems involve coordinated scheduling among the gNodeBs (gNB) aimed at controlling

the transmit power in certain time/frequency resources to reduce the generated interference [6].

At the transmitter end, MIMO introduces spatial degrees of freedom (DoF), whereas the linear minimum mean squared error (MMSE) receiver can suppress parts of the received interference signal by exploiting the interference structure when demodulating the desired signal [7]. MIMO transmission and the MMSE receiver are therefore foreseen to play a prominent role in improving the *spectral efficiency* of future 5G systems [8], [9]. It is well known that utilizing some of the MIMO spatial DoFs for interference suppression instead of transmitting data streams using all spatial DoFs can improve the network performance [10]. With MIMO transceivers and MMSE receivers, interference coordination can further include coordination in the MIMO spatial DoF, i.e., the number of independent transmitted streams or rank.

Rank coordination/adaptation algorithms have recently been investigated for LTE and 5G systems, for example in [11]–[15]. Reference [11] proposes a method to select the rank that maximizes the mutual information given a

target block error rate, considering perfect channel state information (CSI) and no inter cell interference. A number of rank adaptation (RA) algorithms for the LTE and LTE-Advanced (LTE-A) systems are numerically evaluated in [12].

All the algorithms presented in [11] and [12] are based on the signal-to-interference-plus-noise ratio (SINR), which in turn requires knowledge of the interference covariance matrix (ICM). Due to the multitudes of matrix operations involved, estimating the SINR from the ICM requires accurate CSI, and is computationally costly in practice [13], [14]. Low complexity joint precoding matrix and rank selection algorithms based on average channel information across the entire system bandwidth are proposed for the LTE-A system in [13] and [14]. The proposed ICM-based algorithms searches across all possible rank/precoding matrix combinations to select the rank that is expected to deliver the highest throughput.

Most existing rank adaptation algorithms aim at maximizing different performance criteria at the receiver of interest without considering the interference management aspect of rank coordination. As such, they can be *egoistic* rather than being *altruistic* or *interference-aware*. Such myopic transmission is usually not efficient when considering the overall system-level performance [16]. Coordination among interfering cells is therefore necessary to better manage the interference, as exemplified for a multicell system in [15]. Such coordination becomes even more important in systems employing the MMSE receiver, where the number of interfering streams directly impact the interference resilience at the receivers.

The fundamental trade-off between maximizing the spatial multiplexing gain and minimizing the amount of interference generated toward the interfered receivers has been studied from an information-theoretic perspective in [17]. The authors consider a single transmitter coexisting with multiple receivers, and investigate techniques to exploit the multiple antennas at the transmitter to effectively balance between spatial multiplexing gain and interference avoidance at the receiver end. However, the addressed problem is independent of the receiver architecture and is limited to the rank selection at a single transmitter, hence the network-wide rank coordination problem is not addressed in its entirety.

A. CONTRIBUTIONS

In this work, we propose a novel inter-cell interference coordinated rank adaptation framework which integrates coordination among multiple coexisting cells. The interference suppression capability of the MMSE receiver is specifically considered when formulating the rank adaptation problem, which, to the best of our understanding, has not been considered in earlier contributions. More precisely, the proposed algorithm considers the performance at the desired receiver and the impact of the generated interference on the performance of the interfered receivers when deciding the transmission rank. The proposed rank coordination mechanism

utilizes the game-theoretic concept of ‘pricing’ to balance between the spatial multiplexing gain-vs.-interference rejection capabilities. Moreover, instead of relying on the ICM for estimating the post-MMSE SINR, the SINR is estimated through a robust method using results from random matrix theory (RMT), thereby involving fewer parameter estimations as compared to an ICM-based method.

In summary, the following main contributions are addressed in this paper¹:

- Interference suppression capability at the MMSE receiver is considered in the multi-cell rank coordination problem formulation;
- The post-MMSE SINR is estimated using results from RMT, thereby circumventing the need for expensive ICM estimations;
- A game theoretic pricing based interference coordination framework is proposed;
- Finally, centralized and distributed implementations of the proposed algorithm are presented and thoroughly evaluated.

B. ORGANIZATION

The remainder of this paper is organized as follows: the system model, details of the problem formulation and outline of the proposed algorithm are described in Section II. Section III introduces the post-MMSE SINR estimator, followed by the pricing based interference coordination framework in Section IV. Centralized and distributed implementations of the proposed rank adaptation algorithm are detailed in Section V. Finally, numerical results are presented in Section VI, and Section VII concludes the paper.

C. NOTATIONS

Matrices and vectors are respectively denoted by boldface symbols \mathbf{H} (capital) and \mathbf{h} (small letter). $\mathbf{I}_{M \times K}$ denotes the $M \times K$ dimensional identity matrix, while $\mathbb{E}[\cdot]$, $(\cdot)^H$ and $(\cdot)^T$ respectively denotes the Expectation, the Hermitian and the Transpose operator. $\mathcal{CN}(\mu, \sigma^2)$ represents the complex Gaussian distribution with mean μ and variance σ^2 , and $\mathcal{U}(a, b)$ denotes the uniform distribution with support between a and b , where $(a < b)$. \mathbb{C} represents the set of all complex numbers, with $\text{Im}(s)$ denoting the imaginary component of a complex number s . All logarithms are base 2, unless stated otherwise.

II. SYSTEM MODEL

Let us consider a narrowband multi user-MIMO time division duplexed (TDD) system with a number of cells as shown in Figure 1. We assume that L cells share a given time-frequency slot, with at most a single co-channel active user equipment (UE) in each of the selected cells. Since any given time-frequency slot is assumed fully orthogonal, we can limit our analysis to a particular time-frequency slot without loss of generality. The set $\mathcal{L} = \{1, 2, \dots, L\}$ denotes the set of

¹Preliminary results of this work were presented in [18] and [19].

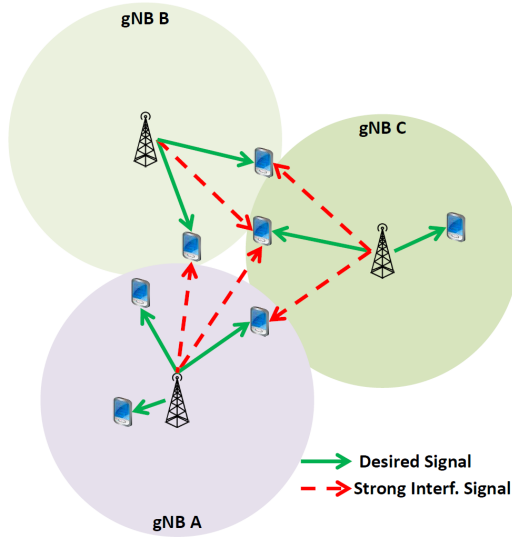


FIGURE 1. Schematic of the considered 5G system model.

all active cells in a given sub-band. As downlink is often the limited link with respect to the interference, we focus on this direction throughout this paper. However the proposed framework can easily be extended to the uplink. Centralized, as well as distributed, rank coordination techniques are discussed in this contribution. The presence of a centralized control node connected to all the cells is assumed for the former discussion. The cells are assumed to be time-synchronized and interconnected via the Xn interface.

Each link in the l^{th} cell is assumed to have N_l transmit antennas and M_l receive antennas. The transmitter-receiver pair in the l^{th} cell communicates by transmitting $d_l \leq \min(M_l, N_l)$ streams over the N_l transmit antennas using an $N_l \times d_l$ linear precoding matrix \mathbf{W}_l .

A. SIGNAL MODEL

The received signal vector \mathbf{y}_l at the receiver in cell l can be expressed as

$$\mathbf{y}_l = \sqrt{\rho_{ll}} \mathbf{H}_{ll} \mathbf{W}_l \mathbf{x}_l + \sum_{k \in \mathcal{L}, k \neq l} \sqrt{\rho_{lk}} \mathbf{H}_{lk} \mathbf{W}_k \mathbf{x}_k + \mathbf{z}_l, \quad (1)$$

where $\mathbf{H}_{lk} \in \mathbb{C}^{M_l \times N_l} \sim \mathcal{CN}\left(0, \frac{1}{2}\right)$ denotes the channel matrix between the k^{th} transmitter and the l^{th} receiver. The vectors $\mathbf{x}_l \in \mathbb{C}^{d_l} \sim \mathcal{CN}\left(0, \frac{1}{2}\right)$ and $\mathbf{z}_l \in \mathbb{C}^{M_l} \sim \mathcal{CN}\left(0, \frac{1}{2}\right)$ represent the transmitted vector from the l^{th} transmitter and the white Gaussian noise vector at the l^{th} receiver respectively. The signal-to-noise ratio (SNR) of the channel between transmitter k and receiver l is given by ρ_{lk} . A block fading channel model is assumed.

1) CSI AVAILABILITY

We assume that the l^{th} transmitter can obtain \mathbf{H}_{ll} by exploiting channel reciprocity. In practice this requires calibration of the transmitter/receiver radio frequency (RF) chains, which

are in general not reciprocal [20]. However, such calibration methods are beyond the scope of this paper and are rather assumed to be in place. Alongside, the long-term channel statistics $\rho_{lk} \forall l, k \in \mathcal{L}$, and the identity of the scheduled active user in each time slot are also assumed to be known. All channel estimations are assumed perfect, unless stated otherwise.

B. CODEBOOK BASED PRECODING

The selection of the precoding matrix \mathbf{W} can either be codebook based where the precoder is chosen from a predefined finite codebook \mathcal{W} , or non-codebook based where it is calculated on the fly based on some knowledge of the CSI. We consider a codebook based system in this work, similar to LTE/LTE-A systems. This enables a smaller feedback overhead and a more predictable interference behaviour compared to a non-codebook based system, and is more suitable for system level implementation [21]. The codebook defined in the LTE standard [22] is considered.

C. SUPPORT FOR MMSE RECEIVER

Considering the signal model presented in (1), the signal of interest at the i^{th} stream of the l^{th} receiver can be decomposed as

$$\begin{aligned} \mathbf{y}_{l,i} = & \underbrace{\sqrt{\rho_{ll}} \mathbf{g}_{ll,i} x_{l,i}}_{\text{desired signal}} + \underbrace{\sqrt{\rho_{ll}} \sum_{j \neq i, j=1}^{d_l} \mathbf{g}_{ll,j} x_{l,j}}_{\text{Intra-stream interf. (ISI)}} \\ & + \underbrace{\sum_{k \neq l, k \in \mathcal{L}} \sqrt{\rho_{lk}} \sum_{j=1}^{d_k} \mathbf{g}_{lk,j} x_{k,j}}_{\text{Inter-cell interf. (ICI)}}, \end{aligned} \quad (2)$$

where $\mathbf{g}_{lk,i}$ is the i^{th} column of the $M_l \times d_k$ -dimensional equivalent channel matrix $\mathbf{G}_{lk} \triangleq \mathbf{H}_{lk} \mathbf{W}_k$, while $x_{l,i}$ is the i^{th} element of \mathbf{x}_l . The desired SINR ($\gamma_{l,i}$) at the i^{th} stream of UE l with the MMSE receiver is given by [23]

$$\gamma_{l,i} = \rho_{ll} \mathbf{g}_{ll,i}^H (\mathbf{I}_{M_l} + \Sigma_{l,i})^{-1} \mathbf{g}_{ll,i}, \quad (3)$$

where $\Sigma_{l,i}$ is the ICM. The corresponding achievable Shannon rate at the l^{th} receiver can then be expressed as

$$R_l = \sum_{i=1}^{d_l} \log(1 + \gamma_{l,i}). \quad (4)$$

It is evident from Eq. (3) that an accurate estimation of the ICM ($\Sigma_{l,i}$) is required for the MMSE receiver operation. In LTE-Advanced, pilot symbols known as the downlink common reference signals (CRS) that are sparsely inserted in the OFDM time-frequency grid can be used to estimate the transmission timing and channel matrices of the interfering cells. The proposal in 5G is to use a specifically designed frame structure to support an accurate ICM estimation [24]. As an example, the 5G frame structure proposed in [25] considers the insertion of a dedicated Demodulation Reference Sequence (DMRS) symbol for enabling channel estimation at

the receiver. Since the cells are synchronized, the transmitted DMRS will overlap, allowing an accurate estimation of the ICM provided orthogonal reference sequences are used.

D. PROBLEM FORMULATION

The achievable rate of the UE in cell l , denoted by R_l , is a function of the precoder matrix \mathbf{W}_l and the transmission rank d_l . An optimization problem for finding the precoding matrices that maximizes the network-wide sum performance measure, subject to a set of given constraints, can be formulated as

$$(P) \begin{cases} \{\mathbf{W}_1^*, \mathbf{W}_2^*, \dots, \mathbf{W}_L^*\} \\ = \arg \max_{\mathbf{W}_l \in \mathcal{W}} \sum_{l \in \mathcal{L}} R_l. \\ \text{s.t. max Transmit Power constraint} \end{cases}$$

The problem is non-trivial since increasing one's own achievable rate by transmitting with a higher rank directly impacts the interference generated at, and subsequently the achievable rate of, the interfered users [26]. Given that the maximization is performed over the predefined set of precoding matrices \mathcal{W} , (P) is a combinatorial problem. Unfortunately, optimally solving such a problem would require a centralized architecture with brute force search over a very large search space (e.g. 64^L combinations for 4×4 MIMO systems with L cells), which is not practically feasible [27], [28]. Alternately, the precoding matrix can be selected by independently searching across all the possible codebook entries at each user and selecting the one that maximizes a given performance measure. However, selecting the precoding matrices independently at each cell results in selfish and myopic transmission strategies that is inefficient from a sum network performance perspective [16], and still computationally exhaustive (e.g., requires $64 \times L$ computations, for the above example [14]).

We therefore propose an efficient distributed sub-optimal solutions of (P). Our approach is to decouple (P) into the following two sub-problems:

$P - 1$: Interference Aware Rank Selection

Interference aware selection of the number of transmission streams (i.e. the dimension d_l of the precoding matrix \mathbf{W}_l),

$P - 2$: Performance Maximizing Precoder selection

Choosing the performance maximizing precoding matrix from the reduced subset within the codebook \mathcal{W} .

The outline of the proposed solutions to the simplified sub-problems are summarized next, followed by detailed descriptions in the remainder of this paper.

E. ALGORITHM OUTLINE

Let us first focus our attention on the sub problem ($P - 1$). It can be observed from Eqs. (3) and (4) that an accurate estimation of the ICM is required in order to calculate the achievable rate. However, the ICM can only be estimated after the actual data transmission, whereas the rank should

be decided prior to the data transmission. This necessitates an efficient and direct SINR estimation method that circumvents the requisite of relying on the ICM for estimating the SINR. We propose to use results from random matrix theory to estimate the SINR. The second challenge associated with sub problem ($P - 1$) is the inter-dependency of the transmission rank and the performance among the co-existing users. Mutual interference makes the user rates coupled, and the overall network objective may not be concave with respect to the transmission rank. The challenge is further exacerbated by the MMSE receiver, whose interference suppress capabilities depend on the strength and the number of the perceived interference streams [29].

To overcome these challenges, we propose to adopt interference pricing as a measure to control the impact of transmitting with multiple ranks. Such interference pricing mechanism has been efficiently used as an interference management technique for power control [30], [31]. Since we have isolated the precoder design as a separate problem, we let $\mathbf{W}_l = \frac{1}{d_l} \mathbf{I}_{M_l \times d_l}$ (the scaling is to enforce maximum power constraint) when considering the sub-problem ($P - 1$). Such a precoding matrix corresponds to one-to-one mapping of the transmitted d_l streams to the first d_l antennas.

Once the transmission rank is decided by solving the sub-problem ($P - 1$), the set of possible precoding matrices reduces to a smaller subset of the matrices with the chosen rank. Hence, the sub-problem ($P - 2$) can be efficiently solved using methods detailed in Section V-C.

III. POST MMSE-SINR ESTIMATION

Let us focus our attention on the i^{th} stream of the l^{th} receiver. Considering the identity matrix precoder, the signal of interest given by Eq. (2) can be rewritten as

$$\begin{aligned} \mathbf{y}_{l,i} = & \underbrace{\sqrt{\frac{\rho_{ll}}{d_l}} \mathbf{h}_{ll,i} x_{l,i}}_{\text{Desired signal}} + \underbrace{\sqrt{\frac{\rho_{ll}}{d_l}} \sum_{j \neq i, j=1}^{d_l} \mathbf{h}_{ll,j} x_{l,j}}_{\text{Inter-stream interference (ISI)}} \\ & + \underbrace{\sum_{k \neq l, k \in \mathcal{L}} \sqrt{\frac{\rho_{lk}}{d_k}} \sum_{j=1}^{d_k} \mathbf{h}_{lk,j} x_{k,j}}_{\text{Inter-cell interference (ICI)}} + \mathbf{z}_l, \end{aligned} \quad (5)$$

where $\mathbf{h}_{lk,i}$ is the i^{th} column of the channel matrix \mathbf{H}_{lk} , while $x_{l,i}$ is the i^{th} element of \mathbf{x}_l . Let us define the sum interference vector at the i^{th} stream of the l^{th} receiver as $\mathbf{u}_{l,i} \triangleq \sqrt{\frac{\rho_{ll}}{d_l}} \sum_{j \neq i, j=1}^{d_l} \mathbf{h}_{ll,j} x_{l,j} + \sum_{k \in \mathcal{L}, k \neq l} \sqrt{\frac{\rho_{lk}}{d_k}} \mathbf{H}_{lk} \mathbf{x}_k$. By assuming the different transmitter sources to be mutually uncorrelated, the covariance matrix of the received interference signal is given as $\Sigma_{l,i} = \frac{\rho_{ll}}{d_l} \sum_{j=1, j \neq i}^{d_l} \mathbf{h}_{ll,j} \mathbf{h}_{ll,j}^H + \sum_{k \in \mathcal{L}, k \neq l} \frac{\rho_{lk}}{d_k} \mathbf{H}_{lk} \mathbf{H}_{lk}^H$.

The post-MMSE SINR of the desired signal can be expressed as² $\gamma = \rho \tilde{\mathbf{g}}^H (\Sigma + \mathbf{I}_M)^{-1} \tilde{\mathbf{g}}$, where $\tilde{\mathbf{g}} \triangleq \frac{1}{d_l} \mathbf{h}_{ll,i}$. Let us consider the eigen-value decomposition (EVD) of Σ as given by $\Sigma = \mathbf{T} \Lambda \mathbf{T}^H$. The M -dimensional diagonal

²The indices are dropped henceforth for ease of presentation.

matrix $\Lambda = \text{Diag}(\lambda_1, \lambda_2, \dots, \lambda_M)$ contains the eigenvalues of Σ , while the m^{th} column of the unitary matrix \mathbf{T} represents the eigenvector corresponding to the eigenvalue λ_m . Using the EVD of Σ , and after some algebraic manipulations, the instantaneous SINR can be re-expressed as [23]

$$\gamma = \rho \sum_{m=1}^M \frac{|\vec{g}_m|^2}{\lambda_m + 1}, \quad (6)$$

where \vec{g}_m is its m^{th} element of the vector $\vec{\mathbf{g}} \triangleq \mathbf{T}^H \tilde{\mathbf{g}}$. Note that, $\tilde{\mathbf{g}}$ and $\vec{\mathbf{g}}$ have the same statistical properties since \mathbf{T} is unitary; i.e. $\vec{\mathbf{g}} \sim \mathcal{CN}(0, \frac{1}{2})$.

In order to circumvent the requisite of relying on the ICM to estimate the post MMSE-SINR, we propose to use the mean SINR expression as an estimate for instantaneous SINR. In particular, we use results from RMT to analyse the asymptotic behaviour of the eigenvalues of Σ appearing in Eq. (6). This allows us to derive a compact analytical expression for the mean SINR that only requires information about the mean interference powers and the rank of each interferer. The proposed SINR estimation method is computationally simpler and involves fewer parameters compared to estimating the ICM itself, e.g., as in [32].

A. DERIVATION OF THE MEAN SINR EXPRESSION

Let us consider the SINR expression given by Eq. (6). By the independence assumption between \mathbf{g} and the eigenvalues λ_m , the mean SINR $\bar{\gamma} \triangleq \mathbb{E}[\gamma]$ can be rewritten as

$$\bar{\gamma} = \frac{\sigma^2}{M} \sum_{m=1}^M \mathbb{E} \left[\frac{1}{\lambda_m + 1} \right]. \quad (7)$$

A direct computation of Eq. (7) requires an M -fold integration over the probability density functions (pdf) of the eigenvalues λ_m , which itself are not readily available. To further circumvent the complexity of this approach, we hypothetically let $M, K \rightarrow \infty$ with the ratio $\beta = \frac{K}{M}$ fixed. In the ensuing asymptotic limit, the distributions of the eigenvalues converge to a non-random distribution [33], thereby reducing Eq. (7) to a single integral. Let $p_{\mathbf{R}}(\lambda)$ denote the said asymptotic distribution. The expression $\bar{\gamma} \triangleq \frac{1}{M} \sum_{m=1}^M \mathbb{E} \left[\frac{1}{\lambda_m + 1} \right]$ appearing in Eq. (7) then converges, in the asymptotic limit, to

$$\bar{\gamma} \rightarrow \int \frac{p_{\mathbf{R}}(\lambda)}{\lambda + 1} d\lambda. \quad (8)$$

In what follows, we present a compact expression for $\bar{\gamma}$.

For completeness of presentation, let us define two integral transforms that are used in the following derivation, namely the *Stieltjes transform* and the *R-transform*.

Definition 1: The Stieltjes transform, $G(s)$, of the random variable x having pdf $p_x(x)$ is defined for $s \in \mathbb{C}$, with $\text{Im}(s) > 0$, as [33]

$$G(s) \triangleq \int \frac{p_x(x)}{x - s} dx. \quad (9)$$

Definition 2: The *R-transform* is defined with the argument $w \in \mathbb{C}$ in terms of the Stieltjes transform as [33]

$$R(w) \triangleq G^{-1}(-w) - w^{-1}, \quad (10)$$

where $G^{-1}(\cdot)$ is the functional inverse of $G(s)$.

A close observation of Eq. (8) and Eq. (9) reveals that $\bar{\gamma}$ is in fact the Stieltjes transform of the ICM Σ evaluated at $s = -1$, i.e. $\bar{\gamma} = G_{\Sigma}(-1)$. It is not straightforward to obtain the pdf of the eigenvalue distribution of the ICM Σ and thereby derive the Stieltjes transform of Σ directly using Eq. (9). To overcome this limitation, we first obtain the R-transform, $R_{\Sigma}(w)$, of the distribution $p_{\Sigma}(\lambda)$. The relationship between the R-transform and the Stieltjes transform can then be utilized to obtain the corresponding Stieltjes transform $G_{\Sigma}(s)$, which in turn can be used to obtain the desired expression for $\bar{\gamma}$ appearing in Eq. (7).

1) R-TRANSFORM OF THE COVARIANCE MATRIX Σ

The covariance matrix Σ , as introduced in Section II, can be written as a sum of the ICMs of the individual interferers. The Gaussian approximation on the matrices \mathbf{H}_j imply that the family of the random matrices $(\{\mathbf{H}_1 \mathbf{H}_1^H\}, \{\mathbf{H}_2 \mathbf{H}_2^H\}, \dots, \{\mathbf{H}_J \mathbf{H}_J^H\})$ is almost surely asymptotically free³ [33]. The R-transform of the sum of random matrices belonging to different sets of a free family is given by the sum of their individual R-transforms. Therefore, we have [33]

$$R_{\Sigma}(w) = \sum_{k=1}^K R_{\Sigma_k}(w), \quad (11)$$

where $R_{\Sigma_k}(w) = \frac{\rho_{lk} \beta_k}{1 - \rho_{lk} w}$, [33] with $\beta_k \triangleq \frac{d_k}{M}$, is the R-transform of the ICM Σ_k from the k^{th} interferer. Note that, for the intra-stream ICM, $\Sigma_l = \frac{\rho_{ll}}{d_l} \sum_{j \neq l, j=1}^{d_l} \mathbf{h}_{ll,j} \mathbf{h}_{ll,j}^H$ and $\beta_l = \frac{d_l - 1}{M}$.

a: Stieltjes TRANSFORM OF THE COVARIANCE MATRIX Σ

The Stieltjes transform of Σ can be evaluated from the R-transform in Eq. (11) by using the following relation as derived from Eq. (10)

$$G_{\Sigma} \left(R_{\Sigma}(-w) - \frac{1}{w} \right) = w. \quad (12)$$

2) EVALUATING $\bar{\gamma}$

As shown earlier, $\bar{\gamma}$ is in fact the Stieltjes transform evaluated at $s = -1$, i.e. $\bar{\gamma} = G_{\Sigma}(-1)$. Thus, the mean SINR expression can be directly obtained from Eqs. (10) and (12) as the solution of the following polynomial equation

$$\sum_{k \in \mathcal{K}} \frac{\rho_{lk} \beta_k}{1 + \rho_{lk} \bar{\gamma}} - \frac{1}{\bar{\gamma}} + 1 = 0. \quad (13)$$

³Free probability theory is to non-commutative random variables (such as matrices) what classical probability theory is to commutative random variables. 'Freeness' in free probability theory is the analogous notion to the central concept of 'independence' in classical probability theory. For more details, please refer to [33] and references therein.

It can be shown that the above polynomial equation admits only one positive root - which is the desired value for $\tilde{\gamma}$ - that can readily be solved using any suitable computational software, e.g. Matlab. Finally, the mean of the post-MMSE SINR in the presence of multiple interferers with unequal interference powers as given in Eq. (7) is obtained in closed form as

$$\tilde{\gamma} = \rho_{II} \tilde{\gamma}. \quad (14)$$

3) VALIDITY AND ROBUSTNESS ANALYSIS

The accuracy of the derived mean SINR expression is numerically validated in this subsection. The analytical mean SINR obtained using Eq. (14) is compared against the simulated numerical sample mean in Figure 2 as a function of the SNR of the desired link (ρ_{II}). The considered scenario involves $K = 10$ interfering cells, where the interference power-to-noise-ratios (INRs) (ρ_{Ik}) are distributed uniformly between -10 and 40 dB. The interferer ranks (d_k) are randomly chosen between 1 and $M (= 4)$ with equal probability. The derived mean SINR is found to match closely with the numerical mean, thereby validating the accuracy of the derived expression.

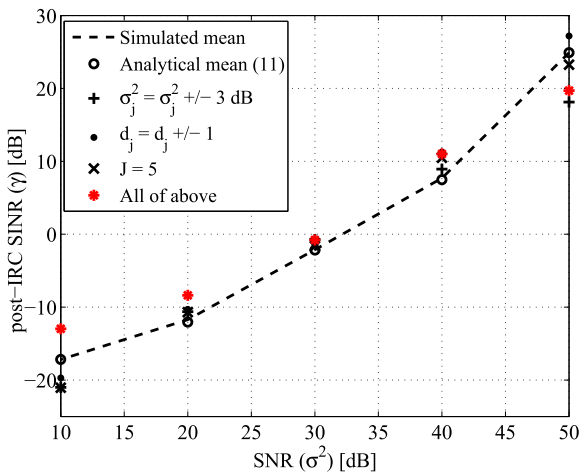


FIGURE 2. Plots for the estimated post-MMSE SINR vs. SNR (ρ_{II}) demonstrating the validity of the proposed SINR estimation method.

We further investigate the impact of estimation non-idealities on the accuracy of the derived mean SINR expression by introducing some non-idealities in the estimated parameters (namely ρ_{Ik} , d_k and K). The plot with the 'plus' (+) marker represents the mean SINRs when the INRs are estimated with an error modelled as a Normal random variable with a variance of 3 dB [34]. The plot with the 'dot' (·) marker shows the mean SINR when the number of interfering streams are estimated erroneously with a margin of ± 1 (i.e. a rank $d_k = 2$ is estimated as $d_k = 1, 2$, or 3 with equal probability). Thirdly, the plot with the 'cross' (×) marker presents the case where the interference contribution from only the 5 strongest interferers is accounted for in the SINR estimate, i.e. when the weaker interference signals

are neglected. Finally the combined impact of all the above errors on the estimated SINR is reflected by the plot with the red marker. The mean SINR with estimation non-idealities is nonetheless found to be within a few dB of the actual (simulated) mean, thereby demonstrating the robustness of the SINR estimation method. The results in further answers any possible question one may have regarding the validity of the asymptotic approach adopted in deriving the mean SINR estimate when the dimensions K and M are small.

IV. PRICING AS AN INTERFERENCE MANAGEMENT CONCEPT

An efficient method to estimate the mean post-MMSE SINR expression as an approximation for the instantaneous SINR has been proposed in the previous section. The next step in solving the sub problem ($P - 1$) is to utilize the derived SINR estimation within an inter-cell interference coordinated rank adaptation framework.

The concept of 'pricing as a control parameter' from game theory is applied in this work to enforce the coexisting users to behave altruistically. In particular, coexisting gNodeBs exchange specific interference aware control information known as *interference price*. Such information allows a transmitter to account for the utility of its transmission in a more comprehensive way by not only considering its own throughput, but also the loss in the interfered users' throughputs resulting from its own transmission [30]. Hence, the rank that is expected to maximize the system level sum throughput can be selected instead of a myopic selection of the rank maximizing the self throughput.

A. EFFECTIVE UTILITY ESTIMATION

When a particular transmitter becomes active, it can achieve a certain throughput under the existing conditions, while simultaneously resulting in a certain amount of interference at the coexisting receivers. With all other conditions unchanged, the additional interference would in turn result in a reduction of the received SINR at the interfered receivers, thereby translating to a reduced throughput. Alongside the achieved throughput at the desired receiver, the dynamics of the resulting interference and its negative impact on the throughput of coexisting users have to be considered in order to fully capture the contribution of the given user to the system sum rate.

The '*effective utility*' measure is introduced in this section to represent the contribution of a particular user to the total system sum rate. It is defined as the difference between the achievable throughput of a particular user and the estimated loss in the achievable throughputs of the interfered users due to the generated interference. Such an utility measure reflects a more socially beneficial utility from a system sum-rate perspective [31].

Deriving the effective utility measure requires estimating the amount of interference generated, and its impact on the throughput performance, at each interfered receiver, as detailed below.

1) ESTIMATING THE THROUGHPUT LOSS DUE TO A CHANGE IN THE INTERFERENCE RANK

Let γ_1 denote the instantaneous SINR of a particular link under a specific channel condition, and $R(\gamma_1) = \log(1 + \gamma_1)$ be the corresponding achievable throughput. Suppose now that a particular interferer changes its transmission rank, resulting in a new SINR and throughput, of γ_2 and $R(\gamma_2)$, respectively. The new throughput $R(\gamma_2)$ can be approximated in terms of the change in the interferer rank (Δd) using the first degree Taylor polynomial [35, eq. (25.2.24)] approximation as

$$R(\gamma_2) \approx R(\gamma_1) + R'(\gamma_1)\Delta d, \quad (15)$$

where $R'(\gamma_1)$ is the derivative of the throughput w.r.t. the interferer rank evaluated at the SINR $= \gamma_1$. The actual throughput loss $Q = R(\gamma_1) - R(\gamma_2)$, can be approximated using Eq. (15) as $Q \approx -R'(\gamma_1)\Delta I$.

2) INTERFERENCE PRICE

The interference price, α_{lk} , is introduced as a measure of the rate of change of the throughput at receiver l w.r.t. the rank from transmitter k , and is defined as $\alpha_{lk} = -\frac{\delta R(\gamma_l)}{\delta d_k}$. Let $\gamma_{l,i}$ be the instantaneous post-MMSE SINR at the i^{th} stream of receiver l . Using the relation $R_l = \sum_i \log(1 + \gamma_{l,i})$, let us further define $\gamma_l = \prod_i (1 + \gamma_{l,i}) - 1$ as the effective SINR at receiver l . Considering the Shannon rate, the interference price at receiver l from transmitter k can be derived as

$$\alpha_{lk} = -\frac{\delta R(\gamma_l)}{\delta \gamma_l} \frac{\delta \gamma_l}{\delta d_k} = \frac{\log(e)}{1 + \gamma_l} \kappa_{lk}, \quad (16)$$

where $\kappa_{lk} = -\frac{\delta \gamma_l}{\delta d_k}$. Directly evaluating κ_{lk} is not straightforward. We therefore propose to approximate κ_{lk} using the mean SINR expression in Eq. (14). Let $\bar{\gamma}_l(d_k)$ be the mean SINR at receiver l considering rank d_k of user k . We can then approximate κ_{lk} as

$$\kappa_{lk} \approx -\frac{\Delta \bar{\gamma}_l(d_k)}{\Delta d_k} = \begin{cases} \bar{\gamma}_l(d_k) - \bar{\gamma}_l(d_k + 1) & d_k < M \\ \bar{\gamma}_l(d_k - 1) - \bar{\gamma}_l(d_k) & d_k = M. \end{cases} \quad (17)$$

3) EFFECTIVE UTILITY

The effective utility measure is a reflection of an individual users contribution to the system sum throughput. Let Q_{kl} be the throughput loss at user k due to the transmission of user l . In other words, isolating the interference from user l result in an additional throughput of Q_{kl} at user k . Following Eq. (15) and using the introduced *interference price* measure, Q_{kl} can be approximated as $Q_{kl} \approx \alpha_{kl}d_l$.

We can thereby define the ‘effective utility’ of a user l as the difference between its achievable desired throughput and the total throughput loss at all the interfered users resulting from the transmission of that particular user. Since the the mean post-MMSE SINR is used as an estimate of the achieved SINR, the estimated SINR per stream (when transmitting with more than one stream) is the same at each streams. Thus the *effective utility* of user l , transmitting with rank d_l can be

defined as

$$\Pi_l(\bar{\gamma}_l, d_l) = d_l \log(1 + \bar{\gamma}_l(d_l)) - \sum_{k \in \mathcal{L}, k \neq l} \alpha_{kl}d_l. \quad (18)$$

where $\bar{\gamma}_l(d_l)$, as given by Eq. (14), is the estimated mean SINR at receiver l considering the desired rank d_l .

V. PROPOSED INTERFERENCE-AWARE RANK SELECTION ALGORITHMS

Having introduced efficient methods to estimate the post-MMSE SINR and the *effective utility* measure, we are now ready to present the proposed interference-aware RA algorithms. First, we present a centralized RA algorithm, followed by a simpler distributed implementation.

A. CENTRALIZED RANK ADAPTATION ALGORITHM

The algorithm outline for a centralized interference-aware RA algorithm for a centralized ultra-dense 5G small cell network is presented in Figure 3. The presented flowchart considers the downlink scenario as a specific example, though the proposed algorithm is equally valid for the uplink direction.

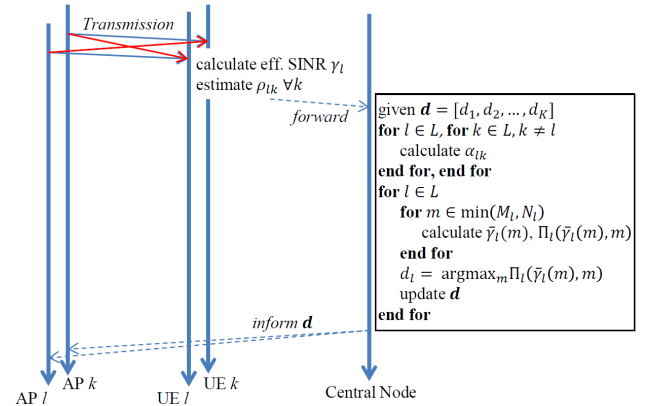


FIGURE 3. Algorithm outline and message flow diagram of the proposed centralized interference-aware rank adaptation algorithm.

At each rank update interval, each UE forwards the effective SINR, along with the interference power measurements from the interfering gNodeBs, to the central node. The mean path loss can be estimated at each receiver, for instance, from the orthogonal reference sequences transmitted by neighbour nodes [36]. In order to minimize the signalling overhead, the UEs can be configured to feedback the mean path loss measurement only if there is a significant change from the previous report. Furthermore, path loss measurements below a certain threshold can be excluded from the reporting since they will have negligible impact for most scenarios.

Given the mean path loss measurements and the available information about the transmission rank, the central node can calculate the interference prices $\alpha_{lk} \forall l, k$ using Eq. (16). The estimated mean post-MMSE SINR $\bar{\gamma}_l(d_l)$ for a candidate transmission rank d_l at a given receiver l can then be calculated using Eq. (14). Note that, the updated transmission

from the current rank adaptation cycle is considered as the transmission ranks of users $1, 2, \dots, l-1$ when calculating $\bar{\gamma}_l(d_l)$ for user l . On the other hand, the transmission rank of the previous RA cycle is considered for the yet-to-be-updated users $l+1, \dots, K$.

The effective utility measure at user l (see Section IV-A) is now ready to be evaluated for each candidate rank $d_l \in \{1, 2, \dots, \min(M_l, N_l)\}$. Finally, the candidate rank that maximizes the effective utility is selected as the transmission rank d_l^* of user l . The proposed centralized algorithm only requires the mean path loss values ρ_{lk} and the received effective SINR γ_l as inputs to the central node. The other parameters (namely the ranks d_l and the interference prices α_{lk}) of the interfering users are obtained from information readily available at the central node. This is in contrast to the complete channel matrix information required for an ICM based rank adaptation approach, such as those presented in [11] and [12].

B. SIMPLIFIED DISTRIBUTED IMPLEMENTATION

There are certain scenarios or network architectures where implementation of the centralized algorithm may not be feasible. A simplified and distributed implementation of the proposed algorithm, as outlined in Algorithm 1, is presented for such scenarios in this section.

Algorithm 1 Proposed Interference-Aware RA Algorithm

Inputs:

At each transmitter l , estimates $\rho_{kl} \forall k \in \mathcal{L}$

Algorithm:

for Each user $l = 1 \dots \mathcal{L}$ **do**

for considered rank, $m = 1 \dots \min(M_l, N_l)$ **do**

 Approximate post-MMSE SINR, $\gamma_{l,m}$ using (14)

 Estimate effective $\Pi_l(m)$ using (19)

end for

 Selected rank $d_j = \arg\max_m \Pi_j(m)$

end for

1) WEIGHTED THROUGHPUT CALCULATION

Instead of the additive ‘interference price as a form taxation’ introduced in Section IV-A, we proposed to introduce a multiplicative interference price that does not require exchange of interference aware control information among the co-existing transmitters. Instead, the key idea is to impose a higher penalty for transmitting with higher ranks, i.e., increasing the number of interfering streams in the system.

Considering a Shannon’s rate achieving idealized modulation and coding scheme for each resource slot, the effective utility of user l transmitting with rank d_l can be re-defined as

$$\Pi_j(d_l) = d_l f(d_l) \log_2(1 + \gamma_l(d_l)), \quad (19)$$

where $\gamma_l(d_l)$ is the estimated mean SINR as given by Eq. (14) and $f(d_l)$ is the penalty imposed for transmitting with rank d_l . ‘Interference-awareness’ is incorporated by defining the weight functions $f(d_l)$ according to the interference

conditions. As an illustrative example, weight functions corresponding to *strong*, *moderate* and *weak* interference scenarios can respectively be defined as

$$f(m) = \begin{cases} \frac{1}{m} & \text{Strong Interference scenario,} \\ \frac{1}{\sqrt{m}} & \text{Moderate Interference scenario,} \\ 1 & \text{Weak Interference scenario.} \end{cases} \quad (20)$$

In general, the choice of the weight function is application and requirement dependent, but must range between the following two extremes: $f(d_l) = 1$ (which implies no penalty) for the *low interference* scenario, to $f(d_l) = 1$ (for rank 1) and $f(d_l) = 0$ (for other ranks), (i.e., transmit with fixed rank one) for the *high interference* scenario.

2) INTERFERENCE ESTIMATION

Similar to choosing the weight function, the interference condition can be determined using different methods. We propose to determine the interference condition at gNodeB l by comparing the sum of the path loss values ρ_{kl} towards the interfered receivers k ($\forall k \in \mathcal{L}, k \neq l$) against the desired SNR ρ_{ll} as shown in Table 1, where $\rho_{l,I} = \sum_{k \in \mathcal{L}, k \neq l} \rho_{kl}$.

TABLE 1. Determining the interference condition.

Condition	Interference Scenario
$\rho_{ll}/\rho_{l,I} > 10$ dB	Weak
$-10 \leq \rho_{ll}/\rho_{l,I} \leq 10$ dB	Moderate
$\rho_{ll}/\rho_{l,I} < -10$ dB	Strong

C. PRECODER SELECTION: SOLVING P – 2

The rationale of decomposing the original optimization problem (P) into two independent sub problems is to simplify the multiuser interference management aspect. We have done so by proposing interference aware rank selection algorithms earlier in this article. The main design criteria for selecting the precoder, i.e., the sub-problem ($P - 2$) is hence to maximize the throughput individually at each receiver, assuming a point-to-point transmission. In other words, ($P - 2$) can be stated as

$$(P - 2) \mathbf{W}_l^* = \arg \max_{\mathbf{W}_l \in \mathcal{W}_l'} R_l, \quad (21)$$

where $\mathcal{W}_l' \subset \mathcal{W}$ is the set of all precoders corresponding to the selected rank d_l^* .

Since the considered Shannon throughput is a monotonically increasing function of the SINR, and assuming a point-to-point transmission, ($P - 2$) is equivalent to solving for the precoder that maximizes the received signal to noise ratio (SNR). Thus, ($P - 2$) in can be reformulated as

$$(P - 2) \mathbf{W}_l^* = \arg \max_{\mathbf{W}_l \in \mathcal{W}_l'} \mathbf{H}_{ll} \mathbf{W}_l \mathbf{W}_l^H \mathbf{H}_{ll}^H, \quad (22)$$

which can be straightforwardly solved, either at the central node (for the centralized implementation) or at the transmitter end (in the distributed case). Note that, such a solution is valid even when the CSI is noisy [37].

VI. NUMERICAL RESULTS

Performance results for the proposed algorithms, obtained through Monte Carlo simulations, are presented in this Section. All results are presented in the form of system sum rate in bps/Hz. A number of cells are simulated, each having a single active UE. The presented results consider terminals with $M = 4$ antennas. A full buffer traffic model [38] is considered for all links. The path loss between any pair of interfering links, more specifically the INRs are chosen randomly from an uniform distribution, the range and support of which is varied to represent different densities of the interfering network.

The presented simulation results are averaged over at least 1000 sample runs to ensure statistical reliability. During each snapshot, the path loss, shadowing and location of devices remain fixed. However these parameters change independently from one snapshot to another.

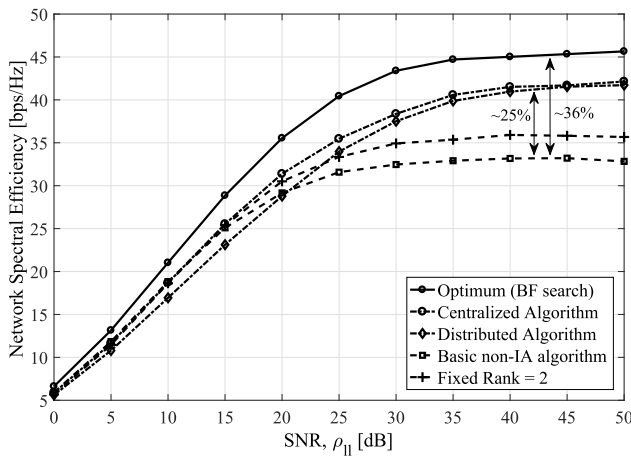


FIGURE 4. Network spectral efficiency in bps/Hz across 6 users for the proposed interference aware RA algorithms with the $SIR \sim \mathcal{U}(30, 0)$ [dB] representing a dense network.

A. IMPACT OF NETWORK INTERFERENCE DENSITY

The sum network spectral efficiency curves for the proposed algorithms under different interference conditions with 6 cells are presented in Figures 4 and 5. Each figure represents a particular interference density scenario and presents results for the proposed centralized and the distributed interference-aware rank adaptation algorithms. The ideally attainable maximum sum rate obtained through brute force (BF) search across the all possible rank combinations is also shown for comparison. Alongside, the performance obtained with a fixed rank 2, and the conventional non interference aware (non-IA) rank adaptation algorithm (such as those presented in [11]–[13] are presented as benchmark results.

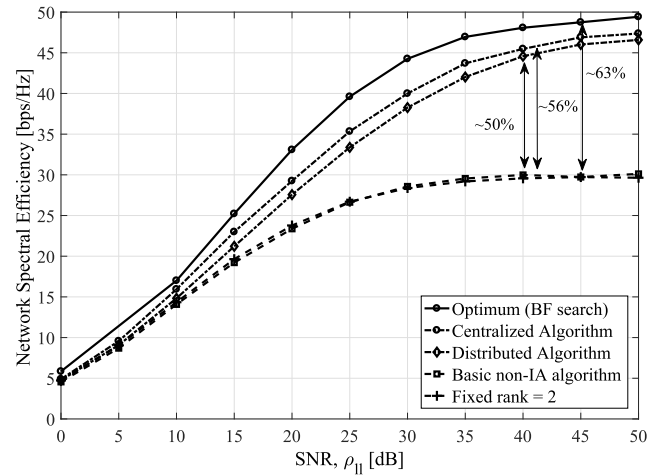


FIGURE 5. Network spectral efficiency in bps/Hz across 6 users for the proposed interference aware RA algorithms with the $SIR \sim \mathcal{U}(40, -10)$ [dB] representing a sparse network where the interferer can at times be stronger than the desired signal.

Observing the performance trends in Figures 4 and 5, the centralized algorithm is found to perform close to the optimum performance. This highlights the fact that the method to estimate the SINR as employed in the proposed RA algorithm, and the interference price as an effective interference control mechanism, are in fact useful in providing a good estimate of the performance of the MMSE receiver. In practice, the BF search optimum performance can only be achieved in the presence of a near-infinite capacity instantaneous feedback link between each user and the central node as it entails centrally available non-causal global CSI. The nominal sum rate gap with the optimum performance can partially be attributed to the fact that the parameters, such as the interference price, are calculated based on the previous transmission time interval parameters, and the approximation involved in estimating the effective interference measure.

On a closer observation, the simplified distributed algorithm is found to perform close to the centralized algorithm under certain scenarios, for example at low (<5 dB) and relatively high (>40 dB) SNR range. However, there is a noticeable performance gap between the performance results of the centralized algorithm compared to that of the distributed algorithm at moderate SNR values (between 5 and 40 dB). The more accurate *interference price* and *effective interference* calculation methods of the centralized algorithm allow better exploitation of the spatial gain vs. interference rejection tradeoff at these practical range of SNR values. On the other hand, the dynamics of the spatial gain-vs.-interference rejection tradeoff are left unexplored when transmitting with a fixed rank as illustrated by the relatively good performance of the fixed rank curves at low SNR values, but not at higher SNR values.

Note that the improved performance of the centralized algorithm comes at an increased computational cost and signalling overhead as discussed in Section V. Therefore, a proper cost-benefit and performance requirement analysis is

necessary when choosing between the centralized and the distributed implementation of the proposed algorithms in practice.

B. IMPACT OF NETWORK SIZE

Next, we investigate the impact of the number of cells in the network. The achieved mean throughput per cell for the proposed algorithms is presented in Figure 6. The SNR of the desired link is fixed at 30 dB, while the interference link strengths are randomly chosen to ensure that the signal to interference ratios (SIR) are follow the uniform distribution $\mathcal{U}(40, -10)$ [dB]. The uniform distribution with a wide range is chosen to model the large interference fluctuation considered in this work. Physically, such a set up can be seen as sparse network where the interferer can at times be stronger than the desired signal, for example due to a closed user group configuration.

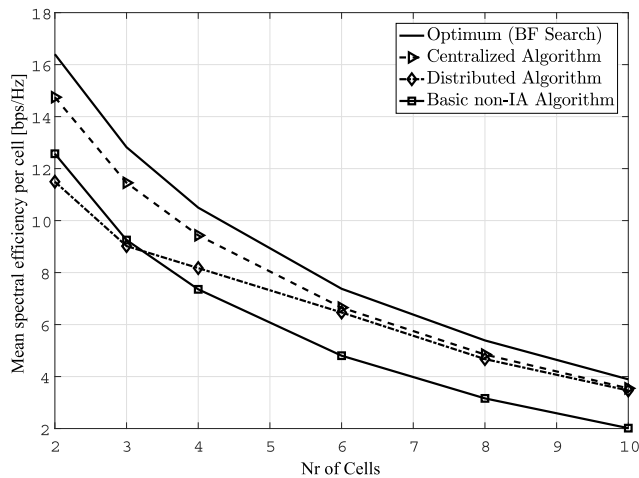


FIGURE 6. Network spectral efficiency per cell with different number of cells for the different proposed algorithms. SNR = 30 dB, SIR $\sim \mathcal{U}(40, -10)$ [dB].

The interference increases with increasing number of active cells, resulting in a decline in the mean rate per cell. For all the considered network sizes, the proposed centralized algorithm performs close to the optimum performance found through BF search. Furthermore, the proposed centralized and distributed algorithms converge in performance with increasing number of cells. This is as expected since with increasing network size, the inter-user interference becomes the dominant performance limiting factor, and hence all algorithms basically converge to transmitting with rank *one*.

For smaller number of cells, the proposed distributed algorithm is found to perform rather poorly, with the basic non-interference aware algorithm outperforming it at very few cells (basically, when number of antennas > number of cells). The observed poor performance is because the interaction among the interfering streams, which is much more intricate with small number of cells, cannot be captured by the simplified weighted penalty measures of the distributed algorithm at sufficient level of accuracy.

C. PERFORMANCE WITH ESTIMATION NON-IDEALITIES

We now investigate the impact of estimation non-idealities on the performance of the proposed algorithm. More specifically, we consider errors in estimating the interference powers (ρ_{lk}) in the mean SINR calculation during the running of the RA algorithm rank selection process. The estimated INR, $\hat{\rho}_{lk}$ is given by $\hat{\rho}_{lk} = \rho_{lk} + \epsilon$ (dB), where the error term ϵ (in dB scale) is a normally distributed error term with zero mean and a variance of 3, i.e. $\epsilon \sim \mathcal{N}(0, 3)$ [34].

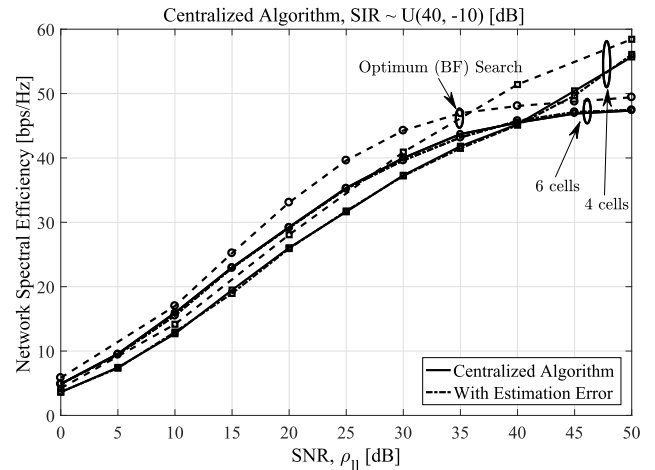


FIGURE 7. Network spectral efficiency performance of the proposed centralized algorithm with, and without estimation non-idealities.

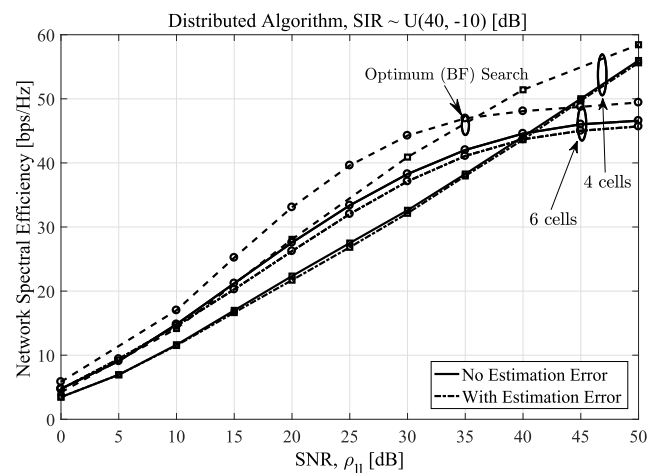


FIGURE 8. Network spectral efficiency performance of the proposed distributed algorithm with, and without estimation non-idealities.

The sum rate performance for the proposed algorithms are presented in Figures 7 and 8, and compared against the optimum performance found through BF search. Results are presented for 4 and 6 cells to demonstrate the impact of the estimation non-idealities for different network sizes. The SIRs are randomly chosen with the uniform distribution $\mathcal{U}(-10, 40)$ [dB]. Alongside the 3 dB estimation error in estimating the INR, we further assume that a fixed interferer rank (of rank = 1) is used instead of accurately estimating the

interferer rank. This is to capture the effects of any possible error in estimating the interferer rank.

The performance of the proposed centralized and distributed rank coordination algorithms are found to be quite robust to the estimation error with negligible performance loss for both of the considered network sizes. The displayed robustness to estimation non-idealities can be attributed to the robustness of the proposed post-MMSE SINR estimation method as discussed in Section III-A.3. It is also interesting to note that the sum rate with four cells outperforms the sum rate with six cells at higher SNR values. With six cells, there are simply not enough spatial DoFs to cancel all the interference sources even when transmitting with a single rank only, since the terminal are equipped with $M = 4$ antennas each. This leads to an interference-limited scenario at higher SNRs, as confirmed by the observed performance saturation in Figure 8. However, with four cells and at high SNRs, each cell can ideally choose to transmit with one stream and use the remaining spatial DoFs to cancel all the interfering streams from the other cells, leading to an interference-free transmission. The resulting performance in that case scales linearly with the log of the SNR, as can be observed from the presented results.

VII. CONCLUSION

We have introduced a novel and practical ‘interference-aware’ rank adaptation algorithm for a 5G system employing the MMSE receiver. The proposed algorithm uses tools from random matrix theory to evaluate the mean post-MMSE SINR, which is one of the parameters used to estimate the achievable rate for each rank combination. Alongside, the concepts of *interference pricing* as a control mechanism, and *effective utility* as an interference-aware measure of the sum throughput are introduced to better reflect the dynamics of the interference-throughput interaction, and to account for the impact of the generated interference on the throughput performance at the interfered receivers.

The selected rank is expected to maximize the sum network throughput. Centralized and distributed implementations of the proposed algorithms are presented, and their respective performance in terms of the system-wide sum throughput are evaluated in details. The proposed algorithms are observed to perform close to the maximum achievable performance obtained through an exhaustive search algorithm for a wide range of network size, while incurring much lower complexity. Furthermore, the proposed algorithms are found to be robust to channel measurement errors and other non-idealities, making them suitable for practical implementation in 5G systems. As part of the future work, we plan to incorporate the different 5G service classes and the concept of multi-connectivity into the proposed inter-cell rank coordination framework.

ACKNOWLEDGEMENT

The authors would like to acknowledge the contributions of their colleagues in the project, although the views expressed

in this contribution are those of the authors and do not necessarily represent the project.

REFERENCES

- [1] J. G. Andrews et al., “What will 5G be?” *IEEE J. Sel. Areas Commun.*, vol. 32, no. 6, pp. 1065–1082, Jun. 2014.
- [2] Y. Niu, Y. Li, D. Jin, L. Su, and A. V. Vasilakos, “A survey of millimeter wave communications (mmWave) for 5G: Opportunities and challenges,” *Wireless Netw.*, vol. 21, no. 8, pp. 2657–2676, Nov. 2015.
- [3] W. Choi and J. G. Andrews, “Spatial multiplexing in cellular MIMO-CDMA systems with linear receivers: Outage probability and capacity,” *IEEE Trans. Wireless Commun.*, vol. 6, no. 7, pp. 2612–2621, Jul. 2007.
- [4] C. Kosta, B. Hunt, A. U. Qudus, and R. Tafazolli, “On interference avoidance through inter-cell interference coordination (ICIC) based on OFDMA mobile systems,” *IEEE Commun. Surveys Tuts.*, vol. 15, no. 3, pp. 973–995, 3rd Quart., 2013.
- [5] D. Lopez-Perez, I. Guvenc, and X. Chu, “Mobility management challenges in 3GPP heterogeneous networks,” *IEEE Commun. Mag.*, vol. 50, no. 12, pp. 70–78, Dec. 2012.
- [6] *Evolved Universal Terrestrial Radio Access Network (EUTRAN); X2 Application Protocol (X2AP), Version-R.8 (Release 8)*, 3GPP, document TS-36.423, Apr. 2010.
- [7] D. N. C. Tse and S. V. Hanly, “Linear multiuser receivers: Effective interference, effective bandwidth and user capacity,” *IEEE Trans. Inf. Theory*, vol. 45, no. 2, pp. 641–657, Mar. 1999.
- [8] F. Boccardi, R. W. Heath, A. Lozano, T. L. Marzetta, and P. Popovski, “Five disruptive technology directions for 5G,” *IEEE Commun. Mag.*, vol. 52, no. 2, pp. 74–80, Feb. 2014.
- [9] N. H. Mahmood, M. Lauridsen, G. Berardinelli, D. Catania, and P. E. Mogensen, “Radio resource management techniques for eMBB and mMTC services in 5G dense small cell scenarios,” in *Proc. IEEE 84th Veh. Technol. Conf. (VTC Fall)*, Montreal, QC, Canada, Sep. 2016.
- [10] R. S. Blum, J. H. Winters, and N. R. Sollenberger, “On the capacity of cellular systems with MIMO,” *IEEE Commun. Lett.*, vol. 6, no. 6, pp. 242–244, Jun. 2002.
- [11] S. Schwarz, C. Mehlh hrer, and M. Rupp, “Calculation of the spatial preprocessing and link adaption feedback for 3GPP UMTS/LTE,” in *Proc. 6th Conf. Wireless Adv.*, Jun. 2010, pp. 1–6.
- [12] Z. Bai et al., “On the physical layer performance with rank indicator selection in LTE/LTE-advanced system,” in *Proc. 21st IEEE PIMRC-Workshop*, Istanbul, Turkey, Sep. 2010, pp. 393–398.
- [13] S. Lei, Y. Xiong, and X. Yang, “Novel method to calculate rank indicator in LTE systems,” in *Proc. Int. Conf. Wireless Commun., Netw. Mobile Comput. (WiCOM)*, Wuhan, China, Sep. 2011, pp. 1–4.
- [14] D. Ogawa, C. Koike, T. Seyama, and T. Dateki, “A low complexity PMI/RI selection scheme in LTE-A systems,” in *Proc. 77th IEEE Veh. Technol. Conf. (VTC Spring)*, Dresden, Germany, Jun. 2013, pp. 1–5.
- [15] B. Clerckx, H. Lee, Y.-J. Hong, and G. Kim, “A practical cooperative multicell MIMO-OFDMA network based on rank coordination,” *IEEE Trans. Wireless Commun.*, vol. 12, no. 4, pp. 1481–1491, Apr. 2013.
- [16] Z. K. M. Ho and D. Gesbert, “Balancing egoism and altruism on interference channel: The MIMO case,” in *Proc. IEEE Int. Conf. Commun. (ICC)*, Cape Town, South Africa, May 2010, pp. 1–5.
- [17] R. Zhang and Y.-C. Liang, “Exploiting multi-antennas for opportunistic spectrum sharing in cognitive radio networks,” *IEEE J. Sel. Topics Signal Process.*, vol. 2, no. 1, pp. 88–102, Feb. 2008.
- [18] N. H. Mahmood, G. Berardinelli, F. M. L. Tavares, M. Lauridsen, P. Mogensen, and K. Pajukoski, “An efficient rank adaptation algorithm for cellular MIMO systems with IRC receivers,” in *Proc. IEEE Veh. Technol. Conf. (VTC)-Spring*, Seoul, South Korea, May 2014, pp. 1–5.
- [19] N. H. Mahmood, G. Berardinelli, F. M. L. Tavares, and P. Mogensen, “A distributed interference-aware rank adaptation algorithm for local area MIMO systems with MMSE receivers,” in *Proc. 11th Int. Symp. Wireless Commun. Syst. (ISWCS)*, Barcelona, Spain, Aug. 2014, pp. 697–701.
- [20] F. Kaltenberger, H. Jiang, M. Guillaud, and R. Knopp, “Relative channel reciprocity calibration in MIMO/TDD systems,” in *Proc. Future Netw. Mobile Summit Conf.*, Florence, Italy, Jun. 2010, pp. 1–10.
- [21] D. J. Love and R. W. Heath, “Limited feedback unitary precoding for spatial multiplexing systems,” *IEEE Trans. Inf. Theory*, vol. 51, no. 8, pp. 2967–2976, Aug. 2005.

- [22] 3GPP, "Evolved universal terrestrial radio access (E-UTRA): Physical channels and modulation," 3rd Generat. Partnership Project, Tech. Rep. TS-36.211 v12.8.0, Dec. 2015, p. R.12.
- [23] S. Verdú, *Multiuser Detection*, 1st ed. New York, NY, USA: Cambridge Univ. Press, 1998.
- [24] K. I. Pedersen, G. Berardinelli, F. Frederiksen, P. Mogensen, and A. Szufarska, "A flexible 5G frame structure design for frequency-division duplex cases," *IEEE Commun. Mag.*, vol. 54, no. 3, pp. 53–59, Mar. 2016.
- [25] P. Mogensen et al., "Centimeter-wave concept for 5G ultra-dense small cells," in *Proc. VTC-Spring Workshop 5G Mobile Wireless Commun. Syst. Beyond (MWC)*, Seoul, South Korea, May 2014, pp. 1–6.
- [26] W. Yu, T. Kwon, and C. Shin, "Multicell coordination via joint scheduling, beamforming, and power spectrum adaptation," *IEEE Trans. Wireless Commun.*, vol. 12, no. 7, pp. 1–14, Jul. 2013.
- [27] D. Gesbert, S. G. Kiani, A. Gjendemsjo, and G. E. Oien, "Adaptation, coordination, and distributed resource allocation in interference-limited wireless networks," *Proc. IEEE*, vol. 95, no. 12, pp. 2393–2409, Dec. 2007.
- [28] S. G. Kiani and D. Gesbert, "Optimal and distributed scheduling for multicell capacity maximization," *IEEE Trans. Wireless Commun.*, vol. 7, no. 1, pp. 288–297, Jan. 2008.
- [29] J. Choi, *Optimal Combining and Detection: Statistical Signal Processing for Communications*, 1st ed. Cambridge, U.K.: Cambridge Univ. Press, 2010.
- [30] J. Huang, R. A. Berry, and M. L. Honig, "Distributed interference compensation for wireless networks," *IEEE J. Sel. Areas Commun.*, vol. 24, no. 5, pp. 1074–1084, May 2006.
- [31] N. H. Mahmood, G. E. Oien, L. Lundheim, and U. Salim, "A relative rate utility based distributed power allocation algorithm for cognitive radio networks," in *Proc. 23rd IEEE Int. Symp. Pers., Indoor Mobile Radio Commun. (PIMRC)*, Sydney, NSW, Australia, Sep. 2012, pp. 136–142.
- [32] M. Lampinen, F. D. Carpio, T. Kuosmanen, T. Koivisto, and M. Enescu, "System-level modeling and evaluation of interference suppression receivers in LTE system," in *Proc. IEEE 75th Veh. Technol. Conf. (VTC Spring)*, Yokohama, Japan, May 2012, pp. 1–5.
- [33] R. R. Müller, "Applications of large random matrices in communications engineering," in *Proc. Int. Conf. Adv. Internet, Process., Syst., Interdiscipl. Res.*, Sveti Stefan, Montenegro, Oct. 2003.
- [34] E. Limpert, W. A. Stahel, and M. Abbt, "Log-normal distributions across the sciences: Keys and clues," *BioScience*, vol. 51, no. 5, pp. 341–352, May 2001.
- [35] M. Abramowitz and I. A. Stegun, Eds., *Handbook of Mathematical Functions: With Formulas, Graphs, and Mathematical Tables*, 9th ed. New York, NY, USA: United States Dept. Commerce, 1964.
- [36] M. Dong and L. Tong, "Optimal design and placement of pilot symbols for channel estimation," *IEEE Trans. Signal Process.*, vol. 50, no. 12, pp. 3055–3069, Dec. 2002.
- [37] A. Narula, M. J. Lopez, M. D. Trott, and G. W. Wornell, "Efficient use of side information in multiple-antenna data transmission over fading channels," *IEEE J. Sel. Areas Commun.*, vol. 16, no. 8, pp. 1423–1436, Oct. 1998.
- [38] P. Ameigeiras, Y. Wang, J. Navarro-Ortiz, P. E. Mogensen, and J. M. Lopez-Soler, "Traffic models impact on OFDMA scheduling design," *EURASIP J. Wireless Commun. Netw.*, vol. 2012, no. 1, p. 61, Feb. 2012.



NURUL HUDA MAHMOOD was born in Chittagong, Bangladesh. He received the M.Sc. degree in mobile communications from Aalborg University (AAU), Denmark, in 2007, and the Ph.D. degree in wireless communications from Norwegian University of Science and Technology, Norway, in 2012. He has been with the Wireless Communication Networks Section at AAU since 2012. He has authored/coauthored over 40 peer-reviewed publications. His current research interests include resource optimization techniques, modeling and performance analysis of wireless communication systems, and full duplex communication. He is currently involved in the EU funded research project FANTASTIC-5G.



KLAUS INGEMANN PEDERSEN received the M.Sc. degree in electrical engineering and the Ph.D. degree from Aalborg University in 1996 and 2000, respectively. He is currently leading the Nokia Bell Labs Research Team, Aalborg, and also a part-time Professor with the Wireless Communications Network Section, Aalborg University. He has authored/coauthored over 150 peer-reviewed publications on a wide range of topics, as well as an inventor on several patents. His current research work is related to 5G design, including radio resource management aspects and end-to-end performance. He is currently involved in the EU funded research project FANTASTIC-5G as a work package leader.



PREBEN MOGENSEN received the M.Sc. and Ph.D. degrees from Aalborg University in 1988 and 1996, respectively. He became a full Professor with Aalborg University in 1999. He has also been holding a part time position at Nokia since 1995. He currently heads the Department of Electronic Systems, Wireless Communication Networks Section. He has supervised more than 35 successfully finalized Ph.D. candidates and has co-authored more than 300 scientific publications. His current research interests include 5G and IoT. He was nominated an NSN Fellow in 2009.

...